Fermilab FERMILAB-CONF-04-503-E CDF DECEMBER 2004

Recent Results in High p_T Physics at CDF II

Soushi Tsuno (CDF Collaboration)
Department of Physics, Faculty of Science, Okayama University
3-1-1 Tsushima-naka, Okayama 700-8530, Japan

Abstract

The Tevatron Run II program has been in progress since 2001. The CDF experiment has accumulated roughly five times as much data as did Run I, with much improved detectors. Preliminary results from the CDF experiment are presented. We focus on recent high p_T physics results in the Tevatron Run II program.

1 Introduction

The CDF (Collider Detector at Fermilab) experiment is a general purpose experiment for the studies of $p\bar{p}$ collisions at the Tevatron Collider, located at the Fermi National Accelerator Laboratory (Fermilab), in Batavia, Illinois, U.S. The Tevatron is the highest-energy accelerator machine in the world. The accelerator [1] and the CDF(D0) [2] detectors have been upgraded since the end of Run I in 1996.

The accelerator complex has added the Main Injector, replacing the old Main Ring, to inject higher intensity beams to the Tevatron and to produce more anti-protons to be used for collisions. The Tevatron center-of-mass energy has been increased from 1.8 TeV in Run I to 1.96 TeV. The instantaneous luminosity has improved steadily since the beginning of Run II. The record value at the time of this conference is 6.3 $\times$ 10^{31} cm^{-2}s^{-1} which is about 3 times higher than the Run I record value and is close to the Run IIa goal of 8.6 $\times$ 10^{31}. The integrated luminosity delivered to each experiment has exceeded 450 pb^{-1}, with about 80% of the delivered luminosity recorded by the detectors. The CDF detector has completely new tracking and forward calorimetry systems, extended muon tracking coverage, and major trigger/DAQ upgrades.

Since the Tevatron Run II program officially started in March 2001, the CDF Collaboration has been extensively exploring new physics beyond the Standard Model (SM). Measuring high p_T phenomena to establish the SM in the electroweak sector is also important in that it may give us knowledge about symmetry breaking in nature. In this paper we describe recent CDF results for high p_T physics.

2 Electroweak Physics

2.1 Production of single gauge bosons

The great success of the Standard Model in the recent decades leaves no doubt that gauge theories are capable of describing the interactions between elementary particles. With the larger collision energy available to probe higher energy scattering events, a high precision measurement may illuminate the observed structure of the families of particles.

The CDF has performed studies of various aspects of the properties of the W and Z electroweak bosons. These are cleanly identified with their decays to leptons (in CDF mostly electrons or muons). The Z boson is identified by using two high p_T lepton candidates within the mass range of the Z boson. The invariant mass distribution for Z boson candidates is shown in Figure 1. The production cross sections are measured to be [3]

$$\sigma(p\bar{p} \to Z/\gamma^* \to l^+l^- + X) = 254.3 \pm 3.3(stat.) \pm 4.3(syst.) \pm 15.3(lumi.) \quad \text{pb},$$

in good agreement with a theoretical prediction of 251.3 $\pm$ 5.0 pb at NNLO level with MRST parton distribution functions (PDF's)[4].

Decays of W bosons are distinguished by one high p_T lepton and missing transverse energy from the (undetectable) neutrino. The transverse mass distribution for W boson candidates is shown in Figure 2, where the transverse mass is given as $M_T = \sqrt{2E_T^l E_T^{missing}[1 - \cos(\Delta\phi^{l-missing})]}$. The production cross

sections are measured to be [3]

$$\sigma(p\bar{p} \to W \to l\nu + X) = 2777 \pm 10(stat.) \pm 52(syst.) \pm 167(lumi.) \quad \text{pb},$$

in good agreement with a prediction of 2687 ± 54 pb at NNLO level with MRST PDF's[4].

In Figure 3, we summarize the single boson production cross sections as a function of the center-of-mass energy, starting from the earlier measurements at CERN together with the previous measurements of Run I. We see good agreement with the theoretical predictions.

The ratio of the Z and W boson production cross sections is used as an indirect measurement of the W boson width. The ratio is defined as

$$R \equiv \frac{\sigma(p\bar{p} \to W \to l\nu + X)}{\sigma(p\bar{p} \to Z/\gamma^* \to l^+l^- + X)} = 10.93 \pm 0.15(stat.) \pm 0.13(syst.).$$

Using a theoretical calculation of the ratio of W and Z production cross sections, and a measured value of the leptonic branching ratio of the Z boson from the LEP experiments [5], we can extract the leptonic branching ratio and total width of the W boson,

$$Br.(W \to l\nu) = 0.1089 \pm 0.0022 \quad , \quad \Gamma_W = 2.071 \pm 0.040 \quad \text{GeV}.$$

This value for the W width is compared to previous measurements and the current world average in Figure 4.

One of the remarkable achievements in the CDF II experiment is that track reconstruction is possible at the trigger level. As a result of this, CDF is able to trigger on tau candidate events. Reconstruction of the tau decay is accomplished by finding an energy cluster in the calorimeter with matching isolated tracks. Individual π^0 particles from the tau decay are reconstructed using detectors embedded in the calorimeter at the depth of the maximum of the electromagnetic shower, and the combined invariant mass of the cluster of tracks and π^0's is required to be less than the mass of the tau. The production cross sections of the Z and the W decaying into tau leptons are measured to be [6]

$$\sigma(p\bar{p} \to Z/\gamma^* \to \tau^+\tau^- + X) = 242 \pm 48(stat.) \pm 26(syst.) \pm 15(lumi.) \quad \text{pb},$$
$$\sigma(p\bar{p} \to W \to \tau\nu + X) = 2.62 \pm 0.07(stat.) \pm 0.21(syst.) \pm 0.16(lumi.) \quad \text{nb}.$$

Lepton universality can be measured with the three generations of lepton family. Calculating the ratio R for each channel separately, we derive the values for the ratios of the coupling constants:

$$\frac{g_\mu}{g_e} = 1.011 \pm 0.018 \quad , \quad \frac{g_\tau}{g_e} = 0.99 \pm 0.04.$$

These are all consistent with the respective SM predictions.

In Z boson production, the forward-backward asymmetry yields measurements of $\sin^2\theta_W$, the couplings with up- and down-type quarks in the proton/antiproton, and a search for higher mass Z' bosons. Note that this is a test unique to the Tevatron. The asymmetry is defined as

$$A_{fb} \equiv \frac{\sigma(\cos\theta > 0) - \sigma(\cos\theta < 0)}{\sigma(\cos\theta > 0) + \sigma(\cos\theta < 0)},$$

where θ is the polar angle between the incoming proton and the outgoing lepton. The distributions of the asymmetry around the Z-pole and in the high mass region are shown in Figure 5 and 6, respectively. Both distributions agree with the SM predictions. Extracting $\sin^2\theta_W$ from these shapes, we can obtain [7]

$$\sin^2\theta_W = 0.2238 \pm 0.0046(stat.) \pm 0.0020(syst.).$$

2.2 Pair production of gauge bosons

An non-abelian gauge theory describing the electroweak interactions induces the three- and four-point self-couplings of gauge bosons. Measurements of the pair production of the gauge bosons is a fundamental

tests for the self-couplings. The cross section for W^+W^- production has been measured in the *dilepton* channel at CDF [8]. The azimuthal angle between the missing transverse energy and the closest lepton is used to enhance the candidate events, and is shown in Figure 7. The measured value is

$$\sigma(p\bar{p} \to W^+W^- \to l^+l^-\nu\bar{\nu} + X) = 14.3^{+5.6}_{-4.9}(stat.) \pm 1.6(syst.) \pm 0.9(lumi.) \quad \text{pb},$$

which is consistent with the SM expectations [9].

Inclusive Wγ and Zγ production is also studied [10]. The photon can be radiated from the initial-state quark and final-state lepton, and from the W boson via the triple gauge coupling. The contribution from the W is enhanced in high E_T region, and so the E_T spectra probes the anomaly to that triple gauge boson coupling. In Figure 8, we show the photon E_T distribution, and no excess is observed. The measured production cross sections are

$$\sigma(p\bar{p} \to W\gamma + X) \cdot Br.(W \to l\nu) = 19.7 \pm 1.7(stat.) \pm 2.0(syst.) \pm 1.1(lumi.) \quad \text{pb},$$
$$\sigma(p\bar{p} \to Z/\gamma^*\gamma + X) \cdot Br.(Z/\gamma^* \to l^+l^-) = 5.3 \pm 0.6(stat.) \pm 0.4(syst.) \pm 0.3(lumi.) \quad \text{pb}.$$

Those results are compared with the NLO calculation [11] of 19.3 $\pm$ 1.3 pb for Wγ production and 5.4 $\pm$ 0.4 pb for Zγ production, and both results are in good agreement with the theoretical calculation. A more direct test of the gauge couplings will be performed when the angular distributions in those events are studied and the radiation amplitude zero is looked for directly.

3 Top Quark Physics

3.1 Overview

Since the discovery of the top quark in 1995 by the CDF and D0 collaborations [12], the study of the properties of the top quark has been the most important mission in the Run II physics program. While the existence of the top quark demonstrates the correctness of the Standard Model, nothing tells us about the hierarchy problem of the mass gap among the quark families and generations.

At the Tevatron, the production mechanism is the creation of a top and and anti-top pair via quark-antiquark annihilation (85%) or via gluon fusion (15%). The top quark is assumed to then immediately decay into a W boson and a bottom quark. The final observed signature thus depends on the decay modes of the W bosons that come from the top and anti-top. The analysis strategy is basically categorized by the *dilepton* ($l^+\nu b l^-\bar{\nu}\bar{b}$, ~5% of all $t\bar{t}$ events), *lepton+jets* ($l\nu bq\bar{q'}\bar{b}$, ~30%), and *all hadronic* ($q\bar{q'}bq\bar{q'}\bar{b}$, ~44%) channels. The analysis is also categorized by the b-tagging algorithms, but only combined results are presented in this section.

3.2 Production cross sections

At CDF, we measure the top pair production cross section in the *dilepton* and *lepton+jets* channels using either counting experiments or by fitting the data to kinematics distributions that can discriminate background from signal. The *all hadronic* channel is also in progress.

The *dilepton* channel uses two leptons with high transverse momentum, missing energy from the undetected neutrinos, and two jets from the b quarks. This channel is relatively clean relative to the other channels, but is statistically limited. The measurement requires two well identified leptons at first. The tight selection criteria are applied for the both leptons. On the other hand, in order to increase the overall signal statistics for the two leptons, the second measurement requires that the selection criteria to identify the second lepton is loosened, while the tight selection applied to the first lepton heavily discriminates against background. Figure 9 shows the jet multiplicity distribution of the candidate events for the selection of one tight lepton plus an isolated track (the loosest form of lepton identification). Both measurements are consistent with one another and the combined result for the production cross section is [13]

$$\sigma(p\bar{p} \to t\bar{t} + X) = 7.0^{+2.4}_{-2.1}(stat.)^{+1.6}_{-1.1}(syst.) \pm 0.4(lumi.) \quad \text{pb},$$

in good agreement with a theory prediction of $6.7^{+0.7}_{-0.9}$ pb at NLO level with assuming a top mass of 175 GeV [14].

The *lepton+jets* channel requires one lepton and three or more jets in the final state. The sample size is larger than the *dilepton* sample, but there is a significant background contamination from the associated production of a W boson with jets. The purity of the sample can be improved by the identification of at least one b-quark jet. We typically use two different b-tagging algorithms. The first one makes use of the long lifetime of the b hadrons to reconstruct a displaced secondary vertex. The second one identifies the soft muon from semileptonic b-decay. The signal-to-noise ratio can be further improved by requiring the scalar sum of the energy in the event, H_T, to be greater than 200 GeV. The production cross section is thus obtained by requiring at least one b-jet tagged by the b-tagging algorithm in lepton plus three or more jets events. The jet multiplicity distribution of these candidate events by the displaced secondary vertex technique with $H_T > 200$ GeV are shown in Figure 10. The excess of events in the bins $N_{jet} \geq 3$ bins is nicely described after the inclusion of the contributions from top. The production cross sections from both b-tagging algorithms are measured to be [15, 16]

$$\begin{aligned} \sigma(p\bar{p} \to t\bar{t} + X) &= 5.6^{+1.2}_{-1.1}(stat.)^{+0.9}_{-0.6}(syst.) \quad \text{pb} \quad \text{(Secondary Vertex)}, \\ &= 5.2^{+2.9}_{-1.9}(stat.)^{+1.3}_{-1.0}(syst.) \quad \text{pb} \quad \text{(Soft Lepton)}. \end{aligned}$$

Instead of counting signal and background events, one can extract the fraction of $t\bar{t}$ events in the lepton + jets sample by fitting one or more kinematic variables in the data to the expected shapes from signal and backgrounds. As already mentioned, the H_T variable is a strong discriminator of signal and backgrounds. Figure 11 shows the H_T distribution with the expected shapes of signal and backgrounds. At least 4 jets are required for the fitting to H_T in this plot. The estimated production cross section is [17]

$$\sigma(p\bar{p} \to t\bar{t} + X) = 4.7 \pm 1.6(stat.) \pm 1.8(syst.) \quad \text{pb}.$$

A summary of the measured $t\bar{t}$ cross section from CDF is presented in Figure 12. Note that there are many other measurements using various different methods [18].

3.3 Top quark mass

A recent combined result of the top quark mass measurements by CDF and D0 collaboration in the Run I experiments is reported to be 178.0 ± 4.3 GeV [19]. Global EW fits place a 95% CL upper bound on the Higgs mass of ∼260 GeV [20]. The precise measurement of the top quark mass will further constrain the mass bound. The Run II goal of the mass measurement is to control the uncertainties to within 2-3 GeV.

The top quark sequentially decays into b-quark and two fermions via the W boson decay which comes from the parent top quark. The CDF measures the top quark mass with the *lepton+jets* and the *dilepton* channels. In both channels, it is crucial to identify the correct configuration of the top quark decay chain. The incorrect assignment of the event kinematics leads mismeasurement of the top quark mass. This can be additional factor for the systematic uncertainty of the mass measurement in addition to that of the background contribution from the other processes. In order to select the event topology to reconstruct the top quark decay chain, the fitting techniques are applied by event-by-event basis. In this case, two W boson resonanse works as strong constrains to the top event topology of the top pair production.

In the *lepton+jets* channel, traditional "template" methods which was used in Run I measures the top quark mass by comparing the reconstructed mass per event with template distributions from the simulated $t\bar{t}$ events of varying masses [21]. The multivariate templates method [22] is used weighting events according to the probability for the chosen jet-parton assignment to be correct. The Dynamical Likelihood Method (DLM) [23] uses the probability formed from the $t\bar{t}$ matrix element to utilize maximal information from the events. This method [24] results in the best value of the top quark mass of

$$M_t = 177.8^{+4.5}_{-5.0}(stat.) \pm 6.2(syst.) \quad \text{GeV}.$$

Figure 13 shows the top mass distribution from the DLM analysis. The systematic uncertainty is dominated by the measurement of jet energies.

In the *dilepton* channel, due to the presence of two neutrinos, one more extra condition driven by the Monte Carlo simulation is imposed on the kinematical variables for the neutrinos. The best fit returns

$$M_t = 168.1^{+11.0}_{-9.8}(stat.) \pm 8.6(syst.) \quad \text{GeV},$$

by the neutrino weighting method [25]. The other top mass measurements using the *dilepton* channel can be seen in [26].

A summary of the top mass measurements from CDF is presented in Figure 14.

3.4 W helicity in top decay

The W boson coming from top decay can be either left-handed (L) or longitudinally (0) polarized. Those fraction to both polarization states is predicted in the Standard Model as

$$f_0 = \frac{\Gamma(t \to bW_0)}{\Gamma(t \to bW_0) + \Gamma(t \to bW_L)} = \frac{M_t^2}{M_t^2 + 2M_W^2} = 0.70,$$

where the b-quark mass is neglected and the top mass is assumed to be 175 GeV. It is important to check the fraction of the longitudinal component, which tells us the symmetry breaking mechanism to give mass to the W boson.

Since the polarization state of the W boson controls the angular distribution of the decaying leptons, CDF has precisely measured the lepton p_T spectra and angular distributions. The estimated f_0 value from those distributions is constrained to be [27, 28]

$$0.25 < f_0 < 0.88 \qquad \text{at } 95\% \text{ C.L.},$$

which is consistent with the Standard Model prediction.

3.5 Search for single top production

Single top production is linked to the direct measurement of the quark mixing in the third generation, $|V_{tb}|^2$, in the CKM matrix [29]. The dominant production mechanics are s-channel Drell-Yan production and the t-channel associated W boson scattering process. Those production cross sections are proportional to $|V_{tb}|^2$. In addition, the measurement of the single top production is also sensitive to new physics; the new charged gauge boson in the s-channel production, anomalous couplings or flavor changing neutral currents in t-channel production.

However, single top events have lower jet multiplicities than those of $t\bar{t}$ production events, so that the analysis of the single top production cross section measurement suffers significant backgrounds from W + jets events in lower jet multiplicity. An optimized search is proposed in [30]. The CDF has searched the single top candidate events, and no candidates are observed. We set a limit of [31]

$$\sigma(p\bar{p} \to tb + X) \quad < 17.8 \quad \text{pb} \qquad \text{at } 95\% \text{ C.L.}.$$

4 Beyond the Standard Model

4.1 Overview

There are several reasons to motivate a new physics beyond the Standard Model: electroweak symmetry breaking, hierarchy problems, the weakness of the gravitational force, and so forth. Those issues inspire new theories beyond the Standard Model such as Supersymmetry (SUSY), Grand Unified Theories (GUT), Technicolor (TC), and Extra Dimensions (ED).

These models predict new experimental signatures with a production cross section small compared to the those of typical QCD processes at the Tevatron. It is often hard to distinguish new phenomena from SM background processes. Jet-based strategies are overwhelmed by the SM processes, so that the CDF has searched lepton-based signatures even through the rates are often suppressed. In this section, only a couple of selected studies are described. Readers may refer to Ref [32] for details.

4.2 Search for narrow resonance in high mass region

A heavy partner of the Z boson, the Z' boson [33], is a by-product predicted by many models of GUT, ED, and little Higgs [34] models. The CDF has searched for an excess in high mass Drell-Yan process using *dilepton* events. The invariant mass distribution of *dilepton* events is shown in Figure 15. No excess is found, and limits are set as a function of the spin state since the experimental acceptance changes depending on the spin state of the resonance particles. Mass limits for the RPV $\tilde{\nu}$ (spin-0), Z' [37, 38, 34, 39] (spin-1), and RS-graviton [40] (spin-2) are set [35].

Events with two jets (*dijet* events) are also used to search for high mass resonance peaks, and limits for some models are set from the measured cross section as shown in Figure 16.

4.3 Search for Higgs boson(s)

With the expected high statistics data from Run II, the CDF and D0 experiments will start reaching sensitivity to production of low-mass Higgs bosons beyond the limits from LEP experiments. The Standard Model Higgs boson predominantly decays into $b\bar{b}$ in the low-mass region. The most promising channel is associated production with a W or Z boson that decays into leptons. In the high-mass region, up to about 180 GeV, Higgs boson production via gluon fusion might be observable in the decay to WW. In a Higgs doublet model, the coupling of the Higgs bosons to b-quarks can be significantly enhanced which allows us to search for the Higgs bosons produced in association with b-quarks. Previous sensitivity studies can be seen in [41, 42].

The CDF has searched for Higgs boson(s) and set cross section limits as a function of Higgs mass in searches for the associated production with a W boson ($l\nu b\bar{b}$) [43], and for the Higgs WW decay mode ($l\nu l\nu$ or $l\nu l\nu l\nu$) [44]. The analysis strategies are the same as for the top quark measurement in *lepton + jets* channel and for the WW cross section measurement. The sensitivity plot is shown in Figure 17. Many other Higgs searches are on-going.

4.4 Search for SUSY in *diphoton + missing* E_T channel

The introduction of supersymmetric particles has many attractive features: the Higgs self-coupling is convergent without fine tuning, all forces except gravity merging at the GUT scale. The introduction of SUSY results in many new particles in TeV region. From the cosmological point of view, SUSY has also been a candidate model for the dark mater. In this section, only a search for the Gauge-Mediated SUSY breaking (GMSB) scenario is described. Many other results are available in Ref. [32].

In GMSB, the second lightest supersymmetric particle (NSLP) is assumed to be the lightest neutralino. And the lightest neutralino can decay into photon and gravitino (LSP). Thus, the final state signature can be two photons and large missing energy. The CDF has looked for this signature. The dominant background source is QCD jet events which make fake missing E_T and photon signals due to the mismeasurement of jets and interaction vertices. After requiring large missing E_T with two identified photons, no candidate is found, and thus we set limits [45],

$$m_{\tilde{\chi}_1^\pm} > 93 \text{ GeV} \quad \text{and} \quad \Lambda > 69 \text{ TeV} \qquad \text{at } 95\% \text{ C.L.},$$

where Λ is the SUSY-breaking scale. The sensitivity plot is shown in Figure 18.

4.5 Search for Leptoquarks

The Leptoquark (LQ) model [46] is a natural consequence from GUT theories. In fact, the relation between quark and lepton quantum numbers can rule out a triangle anomaly [47], so that the theory is renormalizable. Leptoquarks are color triplet bosons carrying both lepton and quark quantum numbers; they can be scalar or vector bosons. At the Tevatron, they can be pair produced through strong interactions and decay either into a charge lepton and a quark ($\beta = 1$) or a neutrino and a quark ($\beta = 0$).

The CDF has searched two scenarios of $\beta = 1$ and $\beta = 0$ for the scalar type Leptoquarks. The signatures are $l^+l^-q\bar{q}$ ($\beta = 1$), $\nu\bar{\nu}q\bar{q}$ ($\beta = 0$), and $l\nu q\bar{q}$ ($\beta = 0.5$) for the first and second generations of

scalar Leptoquarks. The results are shown in Figure 19 and 20 in case of $\beta = 1$ and $\beta = 0$, respectively, and limits are set [48]. A search for the third generation Leptoquark is also in progress.

4.6 Search for Excited Electron

In compositeness models for the substructure of quarks and leptons, the excited states of those particles are considerable [49]. The CDF has searched for excited electrons, e^*, which could be produced through either contact interactions or gauge mediated interactions, and which decays into an electron and photon. The signature would be events with $ee\gamma$ making a mass peak in $M_{e\gamma}$. There is no deviation observed from the Standard Model backgrounds. Upper limits are set at 95% C.L. in the parameter space of the excited electron mass and the M_{e*}/Λ for the contact interaction model or f/λ for the gauge mediated model [50]. Figure 21 and 22 shows the excluded region for the two models, respectively.

5 Conclusion

The Tevatron Run II program has been in progress since 2001. The CDF experiment have accumulated roughly five times more data than in Run I, with much improved detectors. Many physics results have been produced and more are expected in the near future. Preliminary results on the measurements at CDF are presented, most of all will be published in the near future.

In electroweak physics, the production of weak vector bosons has been measured at a new center-of-mass energy. Single W and Z boson production has studied, and some of the properties of the W and Z have been precisely measured. The W boson mass will be measured with the accuracy of 25 MeV with a well-established knowledge of the detector. Pairs of gauge bosons are now being produced in reasonably high statistics, and interactions among gauge bosons will be studied in detail.

For top physics, the top quark measurements have been re-established since the Run I experiment, and new measurements just came out in Run II experiment. The top cross section and mass measurements have improved systematics with various analysis techniques. With large data samples, the top mass will be measured with an accuracy of 2 GeV.

For new physics searches, many results have been improved, resulting in new limits. In the next a few years, the Tevatron is an unique opportunity to directly search for new physics beyond the Standard Model. The CDF is aggressively looking for new phenomena.

Many other studies not fully covered in this paper are on-going. We hope to see many exciting results from the Tevatron.

6 Acknowledgments

The author would like to thank all the people in the CDF Collaboration, and especially Dr. Pasha Murat for assistance in providing information during the Conference. The author would also like to thank the organizers of the Conference.

References

[1] J. Mariner, *et al.*, The Tevatron Run II Handbook, See the www document, http://www-bd.fnal.gov/lug/runII_handbook/RunII_index.html.

[2] R. Blair, *et al.*, The CDF II Detector Technical Design Report, FERMILAB-Pub-96-390-E, November, 1996.

[3] CDF Collaboration, hep-ex/0406078 (2004), submitted to *Phys. Rev. Lett.*.

[4] P.J. Sutton, *et al.*, Phys. Rev. D **45** (1992) 2349;
P.J. Rijken and W.L. van Neerven, Phys. Rev. D **51** (1995) 44;
R. Hamberg, *et al.*, Nucl. Phys. B **359** (1991) 343;
R.V. Harlander and W.B. Kilgore, Phys. Rev. Lett. **88** (2002) 201801.

[5] K. Hagiwara, *et al.*, Phys. Rev. D **66** (2002) 010001.

[6] CDF Collaboration, http://www-cdf.fnal.gov/physics/ewk/latest_results.html .

[7] CDF Collaboration, FERMILAB-Pub-04-314-E (2004), submitted to *Phys. Rev. D.*
[8] CDF Collaboration, http://www-cdf.fnal.gov/physics/ewk/2004/ww/ .
[9] J.M. Compbell and R.K. Ellis, Phys. Rev. D **60** (1999) 113006;
J. Ellison and J. Wudka, Ann. Rev. Nucl. Part. Sci. **48** (1998) 1.
[10] CDF Collaboration, FERMILAB-Pub-04-246-E (2004), submitted to *Phys. Rev. Lett.*.
[11] U. Baur, *et al.*, Phys. Rev. D **48** (1993) 5140;
U. Baur, *et al.*, Phys. Rev. D **57** (1998) 2823.
[12] F. Abe, *et al.*(CDF Collaboration), Phys. Rev. D **50** (1994) 2966; Phys. Rev. Lett. **74** (1995) 2626;
S. Abachi, *et al.*(D0 Collaboration), Phys. Rev. Lett. **74** (1995) 2632.
[13] D. Acosta, *et al.*(CDF Collaboration), Phys. Rev. Lett. **93** (2004) 142001.
[14] N. Kidonakis and R. Vogt, Phys. Rev. D **68** (2003) 114014.
[15] CDF Collaboration, FERMILAB-Pub-04-275-E (2004), submitted to *Phys. Rev. D.*
[16] CDF Collaboration,
http://www-cdf.fnal.gov/physics/new/top/public/ljets/slt/public_200_files/cdf7 174_SLT_200pb-1_public.pdf .
[17] CDF Collaboration,
http://www-cdf.fnal.gov/physics/new/top/confNotes/cdf7154_ttxs_kin_pub.ps .
[18] See CDF Collaboration, http://www-cdf.fnal.gov/physics/new/top/top.html.
[19] The Tevatron Electroweak Working Group, hep-ex/0404010 (2004).
[20] The LEP EW Working Group, http://lepewwg.web.cern.ch/LEPEWWG/
[21] CDF Collaboration, http://www-cdf.fnal.gov/physics/new/top/confNotes/cdf7245_lj _0tag_pub.ps .
[22] CDF Collaboration,
http://www-cdf.fnal.gov/physics/new/top/confNotes/cdf7102_tmass_multivar_-2.p s .
[23] K. Kondo, J. Phys. Soc. Jap. **57** (1988) 4126.
[24] CDF Collaboration,
http://www-cdf.fnal.gov/physics/new/top/confNotes/cdf7056_TopMass_DLM.ps .
[25] CDF Collaboration,
http://www-cdf.fnal.gov/physics/new/top/confNotes/cdf7303_pubTopMass_LTRK_NWA.ps .
[26] See, http://www-cdf.fnal.gov/physics/new/top/confNotes/cdf7194_TopMassDileptonK inemPub.ps
,
http://www-cdf.fnal.gov/physics/new/top/confNotes/cdf7239_dil_template_1.ps .
[27] CDF Collaboration,
http://www-cdf.fnal.gov/physics/new/top/confNotes/cdf7058_top_Whel_pT_public .ps .
[28] CDF Collaboration,
http://www-cdf.fnal.gov/physics/new/top/confNotes/cdf7173_cos_theta_pub_v1_ 0.ps .
[29] N. Cabbibo, Phys. Rev. Lett. **10** (1961) 531;
M. Kobayashi and T. Maskawa, Prog. Theor. Phys. **49** (1973) 652.
[30] Catalin Ciobanu, *et al.*(CDF Collaboration), Phys. Rev. D **69** (2004) 052003.
[31] CDF Collaboration, FERMILAB-Pub-04-340-E (2004), submitted to *Phys. Rev. Lett.*.
[32] CDF II Exotics Group, http://www-cdf.fnal.gov/physics/exotic/exotic.html .
[33] M. Cvetic and S. Godfrey, hep-ph/9504216 (1995).
[34] T. Han, *et al.*, Phys. Rev. D **67** (2003) 095004.
[35] CDF Collaboration,
http://www-cdf.fnal.gov/physics/exotic/r2a/20040916.dilepton_zprime/note_7286. ps .
[36] D. Choudhury, *et al.*, Nucl. Phys. B **660** (2003) 343.
[37] F. Del Aguila, *et al.*, Nucl. Phys. B **287** (1987) 419.
[38] D. London and J.L. Rosner, Phys. Rev. D **34** (1986) 5.
[39] K.D. Lane and S. Mrenna, Phys. Rev. D **67** (1999) 115011.
[40] L. Randall and R. Sundrum, Phys. Rev. Lett. **83** (1999) 3370.
[41] M. Carena, *et al.*, Report of the Higgs working group of the Tevatron Run II SUSY/ Higgs workshop, hep-ph/0010338 (2000).

[42] CDF and D0 Collabration, Results of the Tevatron Higgs Sensitivity Study, FERMILAB-Pub-03-320-E (2003).
[43] CDF Collaboration, http://www-cdf.fnal.gov/physics/exotic/r2a/20040722.lmetbj_wh_tc/note_7126.ps .
[44] Sunny Chuang (CDF Collaboration), Search for Higgs in WW decays at CDF, presented at PHENO2004, Apr. 26-28, 2004.
[45] CDF Collaboration, http://www-cdf.fnal.gov/physics/exotic/old.pub_notes/cdf7162_gmsb_ggmet_pub. pdf .
[46] J. Blümlein, *et al.*, Leptoquark Pair Production in Hadronic Interactions, hep-ph/9610408 (1996).
[47] E.A. Kuraev, *et al.*, Sov. J. Nucl. Phys. **51** (1990) 1031; T.V. Kukhto, *et al.*, Nucl. Phys. B **371** (1992) 567.
[48] CDF Collaboration, FERMILAB-Pub-04-303-E (2004), submitted to *Phys. Rev. Lett.*.
[49] U. Baur, *et al.*, Phys. Rev. D **42** (1990) 815.
[50] CDF Collaboration, FERMILAB-Pub-04-287-E (2004), submitted to *Phys. Rev. Lett.*.

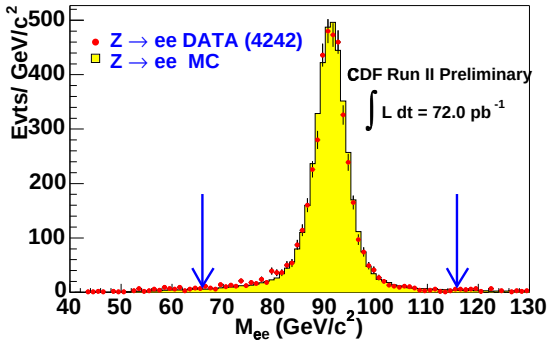

Figure 1: Invariant mass distribution of lepton pairs for $Z \to e^+e^-$ candidates.

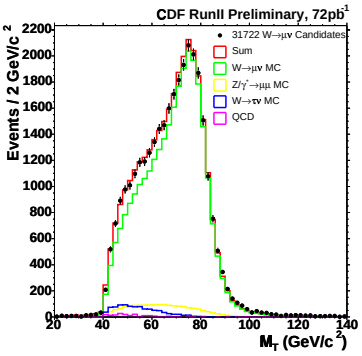

Figure 2: Transverse mass distribution of lepton and missing E_T system for $W \to^{\tau} e\nu$ candidates.

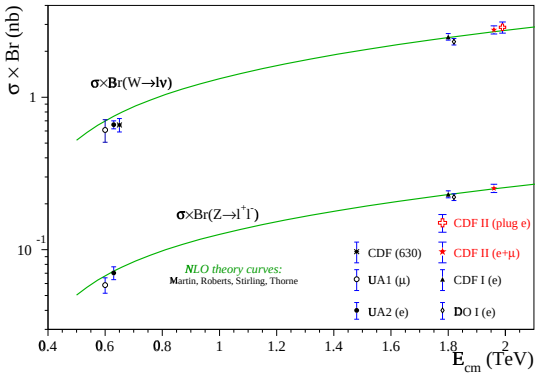

Figure 3: Production cross sections of Z and W bosons as a function of collision center-of-mass energy.

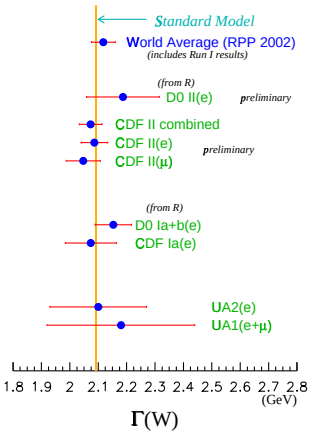

Figure 4: W boson width measurements.

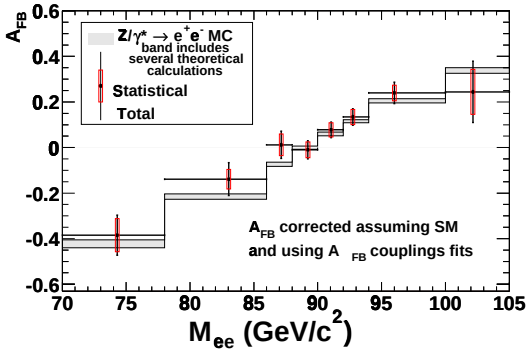

Figure 5: Asymmetry distribution of $Z \to e^+e^-$ events around Z-pole.

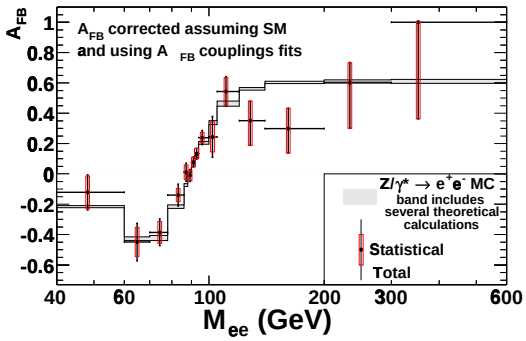

Figure 6: Asymmetry distribution of $Z \to e^+e^-$ events in high mass region.

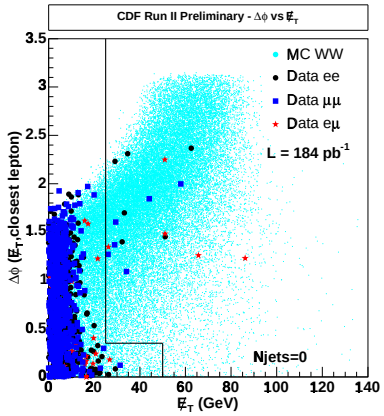

Figure 7: Azimuthal angle between the missing transverse energy and the closest lepton.

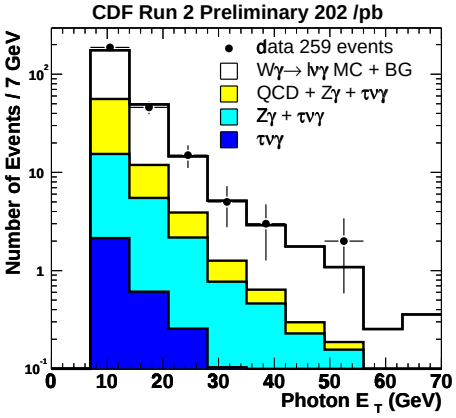

Figure 8: Photon transverse momentum for Wγ production.

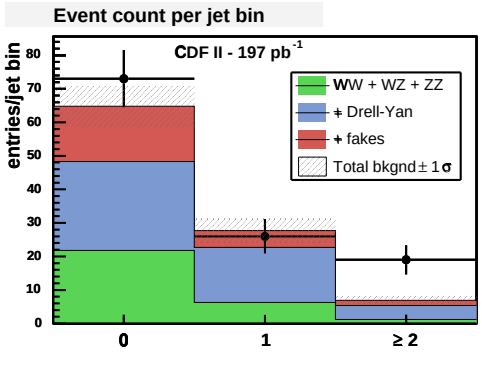

Figure 9: Jet multiplicity distribution of top candidate events in the *dilepton* channel (Lepton+track).

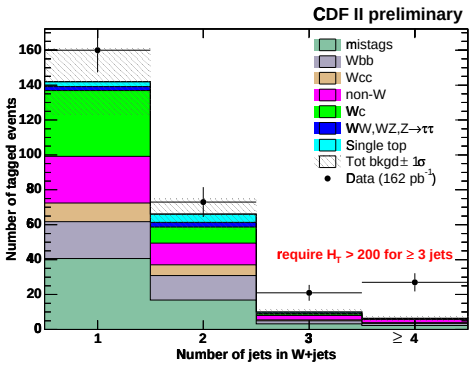

Figure 10: Jet multiplicity distribution of top candidate events in the *lepton+jets* channel with Secondary Vertex b-tagging.

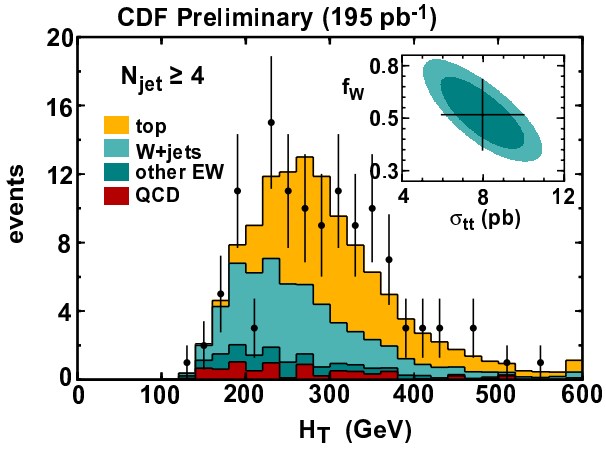

Figure 11: H_T distribution with the expected shapes of signal and backgrounds.

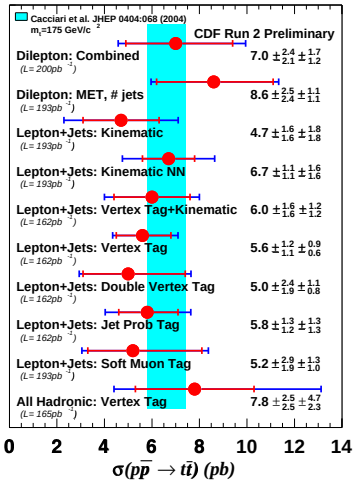

Figure 12: Summary of the measured $t\bar{t}$ cross section from CDF.

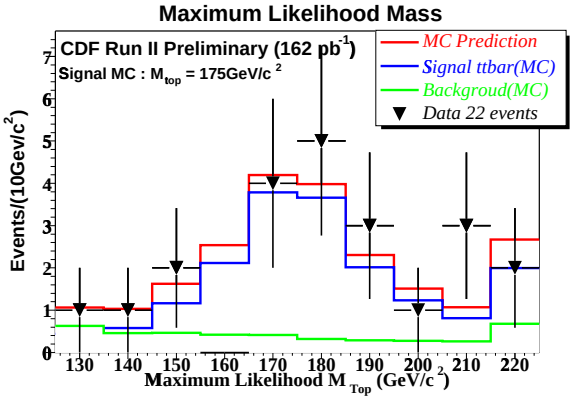

Figure 13: Maximum likelihood mass distribution by DLM analysis.

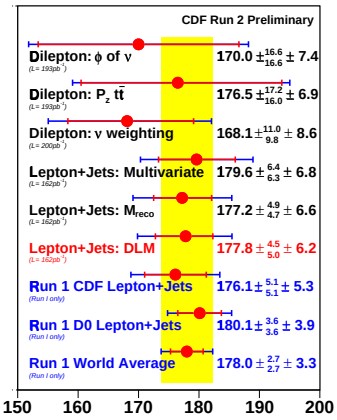

Figure 14: Summary of the measured top mass from CDF.

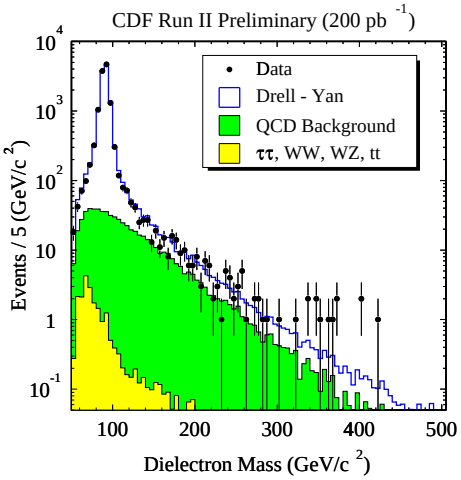

Figure 15: Invariant mass distribution of *dilepton* events.

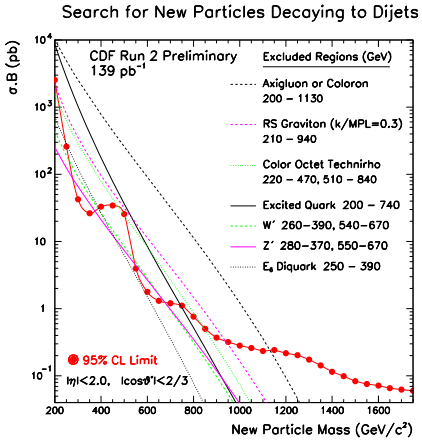

Figure 16: The 95% C.L. upper limit on the cross section times branching ratio for new particles decaying *dijet* for various models.

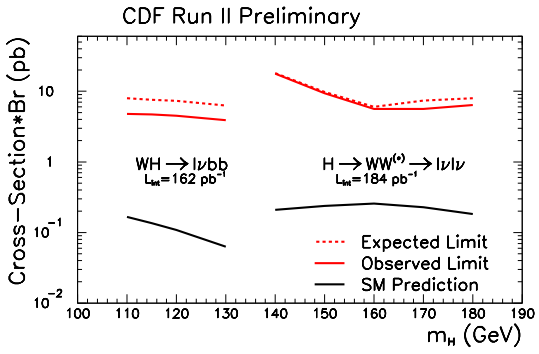

Figure 17: Cross section times branching ratio limit as a function of SM Higgs boson mass.

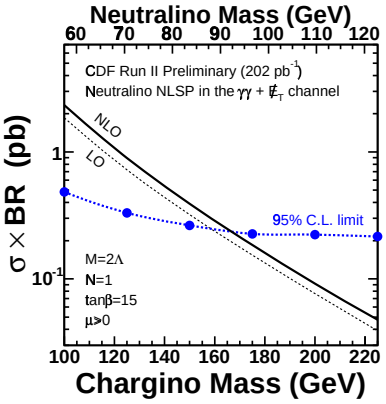

Figure 18: Cross section times branching ratio limit as a function of chargino mass.

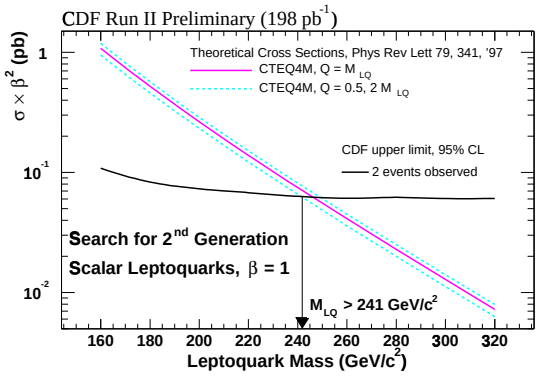

Figure 19: Upper limit on the cross section times squared branching ratio for scalar leptoquark production ($\beta = 1$).

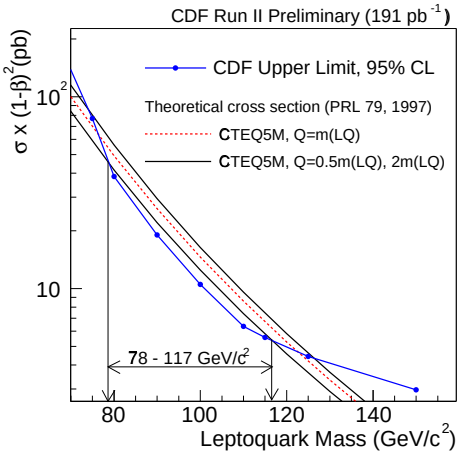

Figure 20: Upper limit on the cross section times squared branching ratio for scalar leptoquark production ($\beta = 0$).

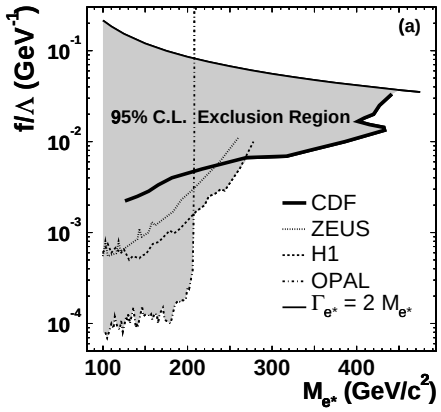

Figure 21: The 95% C.L. excluded region in the parameter space of the gauge-mediated model.

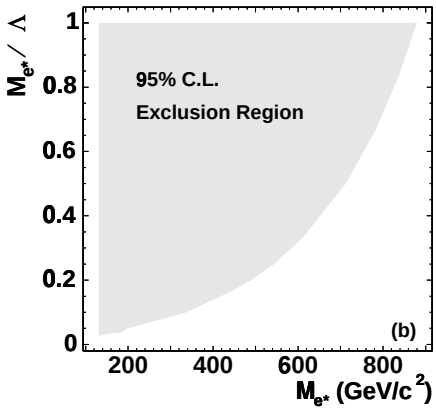

Figure 22: The 95% C.L. excluded region in the parameter space of the contact interaction model.